Neuron
Article

Timing-Dependent Septal Cholinergic Induction of Dynamic Hippocampal Synaptic Plasticity

Zhenglin Gu[1] and Jerrel L. Yakel[1,*]
[1]Laboratory of Neurobiology, National Institute of Environmental Health Sciences, National Institutes of Health, Department of Health and Human Services, Research Triangle Park, NC 27709, USA
*Correspondence: yakel@niehs.nih.gov
DOI 10.1016/j.neuron.2011.04.026

SUMMARY

Cholinergic modulation of hippocampal synaptic plasticity has been studied extensively by applying receptor agonists or blockers; however, the effect of rapid physiological cholinergic stimuli on plasticity is largely unknown. Here, we report that septal cholinergic input, activated either by electrical stimulation or via an optogenetic approach, induced different types of hippocampal Schaffer collateral (SC) to CA1 synaptic plasticity, depending on the timing of cholinergic input relative to the SC input. When the cholinergic input was activated 100 or 10 ms prior to SC stimulation, it resulted in α7 nAChR-dependent long-term potentiation (LTP) or short-term depression, respectively. When the cholinergic stimulation was delayed until 10 ms *after* the SC stimulation, a muscarinic AChR-dependent LTP was induced. Moreover, these various forms of plasticity were disrupted by Aβ exposure. These results have revealed the remarkable temporal precision of cholinergic functions, providing a novel mechanism for information processing in cholinergic-dependent higher cognitive functions.

INTRODUCTION

Modulatory transmitters, such as acetylcholine (ACh), dopamine, and serotonin, play a pivotal role in mediating higher cognitive functions, including learning and memory (Reis et al., 2009). Thus, their modulation of synaptic plasticity, a cellular model of learning and memory, has been extensively studied. However, the vast majority of knowledge is derived from the use of exogenously applied receptor agonists or blockers. The information about the timing and context of neurotransmitter action is usually lacking, and yet this is critical for information processing and computation (Silberberg et al., 2004; Dan and Poo, 2004; Gradinaru et al., 2010). For example, small shifts in the timing of the same glutamatergic input could result in either long-term potentiation (LTP) or depression in the case of spike timing-dependent plasticity (Zhang et al., 1998). Although the modulatory transmitters are generally considered to mediate slow synaptic transmission (Greengard, 2001), studies have shown that the timing of exogenously applied ACh is important in modulating high-frequency stimulation (HFS)-induced hippocampal synaptic plasticity (Ji et al., 2001; Ge and Dani, 2005), suggesting the potential capability of this neurotransmitter to execute physiological functions with high temporal precision.

Here, we have addressed this question by taking advantage of the identifiable cholinergic input pathway from the septum to the hippocampus (Cole and Nicoll, 1983, 1984; Dutar et al., 1995; Widmer et al., 2006; Wanaverbecq et al., 2007; Zhang and Berg, 2007), and the recently developed optogenetic approach (Tsai et al., 2009; Witten et al., 2010) that allows precise control of specific cholinergic input with high temporal precision. We studied how septal cholinergic inputs, activated either by electrical stimulation or via an optogenetic approach, can regulate the synaptic strength of hippocampal Schaffer collateral (SC) to CA1 synapses. The hippocampal SC to CA1 synapses are among the most studied for synaptic plasticity (Malenka, 2003), a widely recognized cellular model for learning and memory (Bliss and Collingridge, 1993). The hippocampus receives the majority (up to 90%) of its cholinergic inputs from the medial septum via the fimbria/fornix, which enters the hippocampus through the stratum oriens (SO) (Dutar et al., 1995). Alterations of cholinergic function in the hippocampus have been implicated in cognitive dysfunction in Alzheimer's disease (AD), schizophrenia, and nicotine addiction (Kenney and Gould, 2008). Understanding how the septal cholinergic input functions in the hippocampus will provide insight not only for understanding higher brain functions but also for the treatment of these disorders.

As opposed to the previous findings that modulatory neurotransmitters have modulatory effects on preexisting HFS-induced synaptic plasticity (Jerusalinsky et al., 1997; Power et al., 2003; Dani and Bertrand, 2007; Kenney and Gould, 2008), here, we report that single pulses of the septal cholinergic input, activated either by electrical stimulation or more precisely by an optogenetic approach, can directly induce different forms of hippocampal SC to CA1 synaptic plasticity, depending on the timing of cholinergic input relative to the SC input, with a timing precision in the millisecond range. Moreover, these different forms of plasticity are differentially impaired in an AD model, a disorder of dementia featured with cholinergic dysfunction (Bartus et al., 1982; Terry and Buccafusco, 2003). Thus, these results have revealed the high temporal precision of cholinergic transmission and its importance in inducing different types of hippocampal synaptic plasticity, providing a novel information-processing mechanism underlying higher cognitive functions that involve the hippocampus and cholinergic transmission.

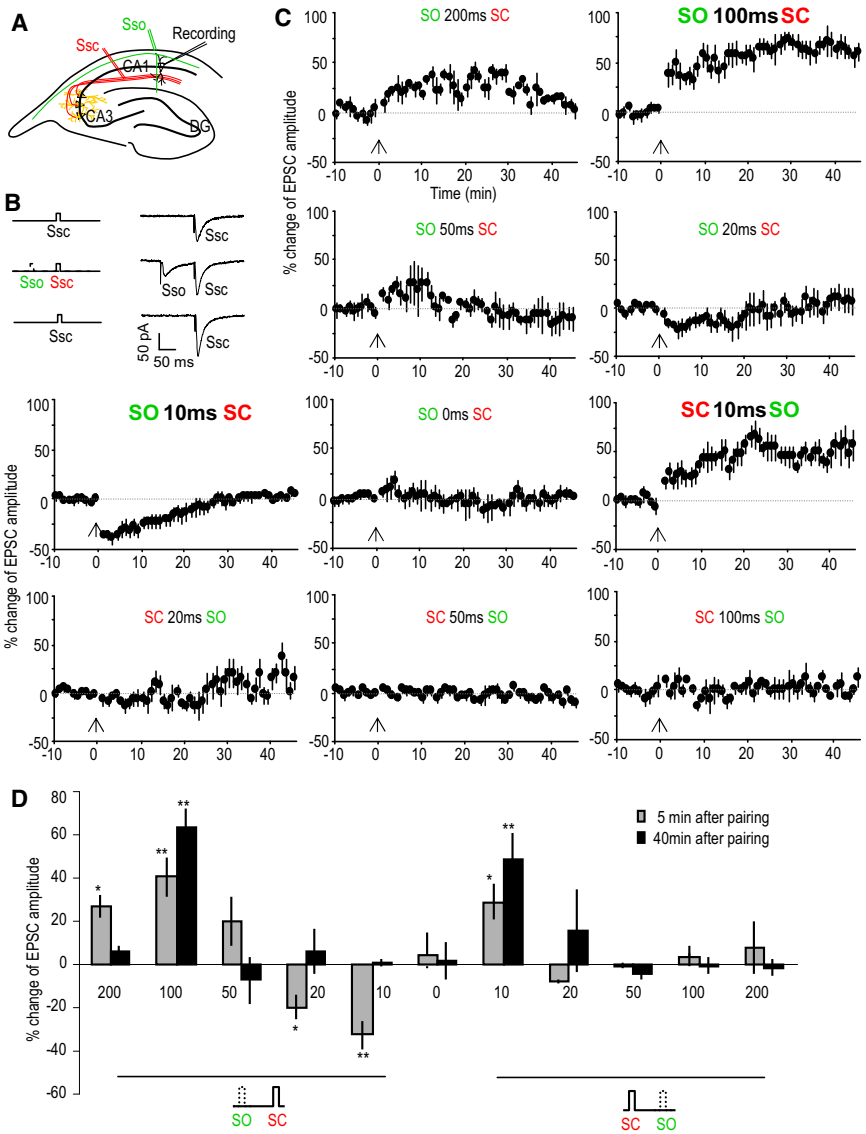

Figure 1. SO Stimulation Induces Various Types of Synaptic Plasticity of SC-CA1 Synapses

(A) Schematic diagram showing the placement of recording and stimulating electrodes in the hippocampal slice. EPSCs were recorded from CA1 pyramidal neurons (Recording) by electrically stimulating the SC pathway (Ssc, in red). Cholinergic inputs were activated by electrically stimulating the SO (Sso, in green). (B) Schematic diagram and sample EPSC traces showing the pairing of SC with SO (middle traces). The SC-EPSCs before (upper traces) and after the pairing protocol (lower traces) were monitored and analyzed. (C) Percent (%) change of SC-EPSC amplitude after pairing with the SO (introduced at the 0 min time point as indicated by the arrows) as compared with that before paring. Different types of plasticity were induced depending on the interval and the order of SC-SO pairing. (D) Bar graph showing the percent (%) change of SC-EPSC amplitude 5 or 40 min after the pairing as compared with the baseline before the pairing. *$p < 0.05$, **$p < 0.01$, as compared with before pairing protocol, Student's t test (n = 5–7 in each group). Data are shown as mean ± SEM. See also Figure S1.

RESULTS

Septal Cholinergic Inputs Induce Dynamic Hippocampal Synaptic Plasticity in a Timing- and Context-Dependent Manner

The SC-CA1 synaptic strength was monitored by recording whole-cell excitatory postsynaptic currents (EPSCs) from CA1 pyramidal neurons by electrically stimulating the SC pathway with single stimulation pulses in hippocampal slices (Figure 1A). Endogenous ACh release was induced by electrically stimulating the SO layer, where cholinergic inputs from medial septal nuclei enter the hippocampus (Cole and Nicoll, 1983, 1984; Dutar et al., 1995; Widmer et al., 2006; Wanaverbecq et al., 2007; Zhang and Berg, 2007). Stimulation of the SO alone, with either single pulses or with high-frequency (HFS) or theta burst (TBS) stimulation, produced no significant change of the SC-CA1 EPSC amplitude (see Figures S1A–S1D available online). In contrast a pairing protocol that combined a single stimulation pulse of the SO with that of the SC (Figure 1B), repeated ten times at 0.033 Hz, resulted in an immediate change of the size of the synaptic response. This effect was temporally dependent in that by varying the time interval and order of the stimulations, the pairing resulted in various forms of synaptic plasticity of the SC-CA1 synaptic transmission (Figures 1C and 1D).

When pairing SO stimulation 100 ms before the SC stimulation, robust LTP of the EPSC amplitude was induced; intervals of 200 and 50 ms were less effective and only produced a short-term potentiation (STP; Figures 1C and 1D). When the interval was shortened to 10 ms, short-term depression (STD) was induced with a less significant effect at a duration of 20 ms. Concurrent stimulation of the SO and SC did not induce any changes in the synaptic response. However, when the SO stimulation was given after the SC stimulation, LTP was induced at the 10 ms time interval, with a slight potentiation at 20 ms and no effect at 50, 100, or 200 ms intervals (Figures 1C and 1D). Interestingly, whereas only five pairings were almost as effective as ten when using ±10 ms intervals (SO before or after SC), five pairings induced only STP instead of LTP when pairing SO 100 ms before SC (Figures S1E–S1H). The induction of different forms of plasticity stresses the importance of the timing of cholinergic inputs and local synaptic activity in inducing this type of synaptic plasticity.

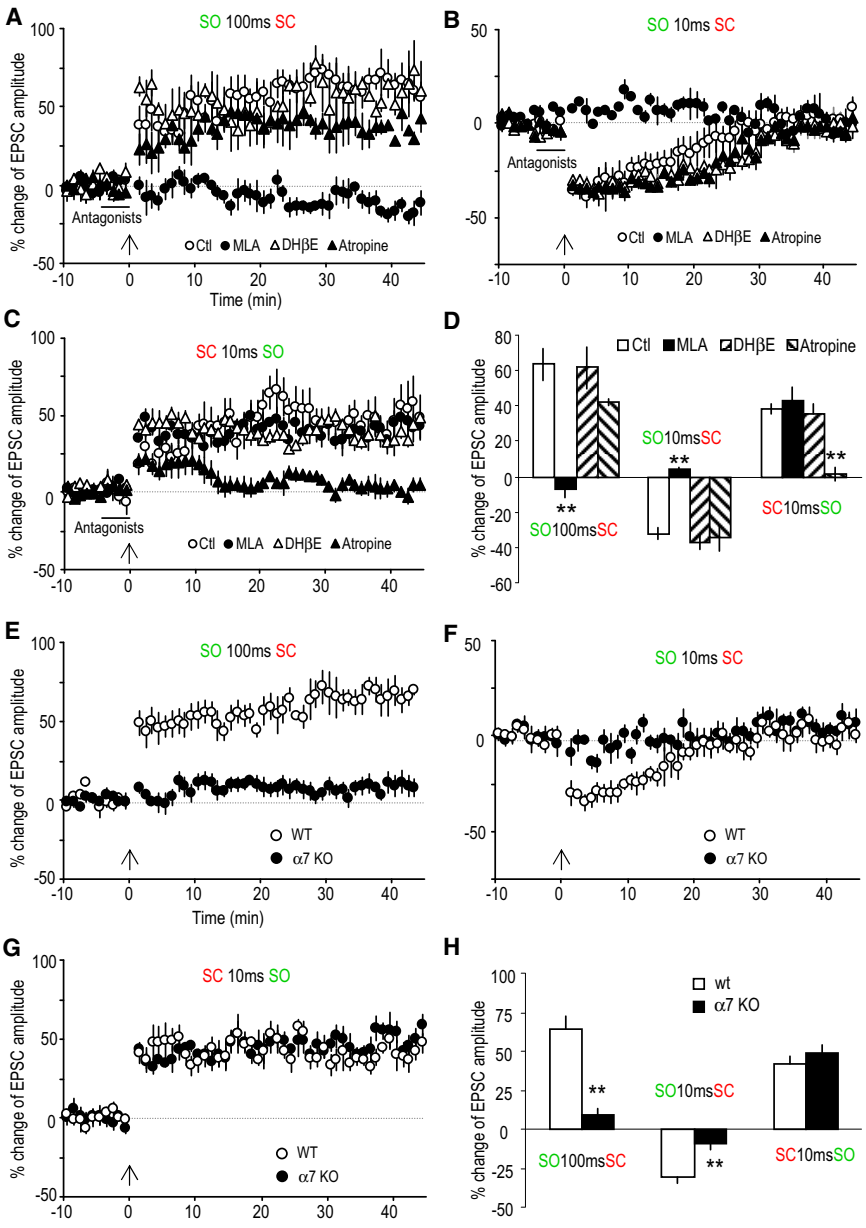

Figure 2. Involvement of α7 nAChRs and mAChRs in Mediating Synaptic Plasticity

(A–C) Percent (%) change of EPSC amplitude showing the effects of three cholinergic antagonists on the three types of plasticity. (A) The LTP induced by pairing the SO 100 ms before the SC was completely blocked by the α7 nAChR antagonist MLA (10 nM), but not by the non-α7 nAChR antagonist DHβE (1 μM) or the mAChR antagonist atropine (5 μM). (B) The STD induced by pairing the SO 10 ms before the SC was also completely blocked by MLA, but not by DHβE or atropine. (C) The LTP induced by pairing the SC 10 ms before the SO was blocked by atropine, but not by MLA or DHβE. (D) Bar graph showing the effects of these three cholinergic antagonists on the three types of synaptic plasticity. Data are shown as mean ± SEM. (E–G) Percent (%) change of EPSC amplitude showing the difference in inducing synaptic plasticity in wild-type (WT) and α7 nAChR KO mice. (E) LTP was induced by pairing the SO 100 ms before the SC in WT, but not the α7 KO mice. (F) STD was induced by pairing the SO 100 ms before the SC in WT, but not α7 KO mice. (G) The LTP induced by pairing the SC 10 ms before the SO was not affected in the α7 KO mice. (H) Bar graph showing the difference between WT and α7 KO mice. $^{**}p < 0.01$, as compared with WT, Student's t test (n = 5–6). Data are shown as mean ± SEM.

This plasticity depends on both the timing of the cholinergic input and the activity of local hippocampal synapses receiving the input. Thus, one cholinergic input may result in different types of plasticity at different synapses, depending on the local glutamatergic activity in each spine. Thus, this timing- and context-dependent mechanism provides not only temporal but also spatial precision.

α7 Nicotinic ACh Receptor and Muscarinic AChR Are Involved in Different Types of Hippocampal Synaptic Plasticity, through Presynaptic or Postsynaptic Mechanisms

To investigate which AChRs might be involved in mediating these forms of plasticity, bath application of cholinergic receptor antagonists was used during the pairing protocol (Figures 2A–2D); MLA and DHβE were used to test for the α7 and non-α7 nAChRs, respectively, and atropine was used to test for the mAChR (Figures 2E–2H). The LTP induced by the preceding SO stimulation (100 ms) was completely blocked by MLA (10 nM), whereas DHβE (1 μM) and atropine (5 μM) were ineffective (Figure 2A). Similarly, the induction of STD by SO 10 ms before SC was also blocked by MLA, with DHβE and atropine also having no effect (Figure 2B). Therefore, induction of either LTP or STD with prior SO stimulation was due to activation of the α7 nAChR. In contrast the LTP induced when the SO stimulation occurred *after* (10 ms) SC stimulation was insensitive to blockade of nAChRs but was blocked by the mAChR antagonist atropine (Figure 2C), indicating that mAChRs mediated this form of plasticity.

The α7 nAChR knockout (KO) mouse was used to further verify the critical role for this receptor in the cholinergic induction of synaptic plasticity. We observed that the LTP and STD induced by SO preceding SC stimulation, which were sensitive to MLA, were entirely absent in slices from the α7 nAChR KO mice, although we observed the plasticity in the wild-type littermates (Figures 2E and 2F). Furthermore, as expected, the mAChR-dependent LTP was unchanged in the α7 nAChR KO mice (Figure 2G).

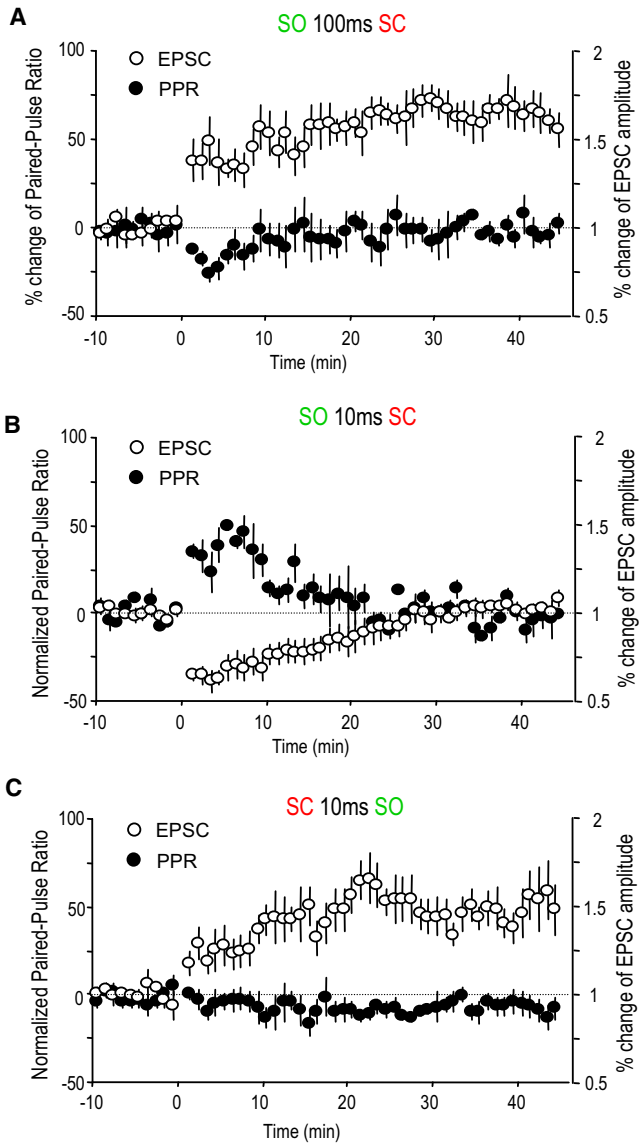

Figure 3. Both Presynaptic and Postsynaptic Mechanisms Are Involved in the SO-Induced Synaptic Plasticity

(A–C) Percent (%) change of PPR and EPSC amplitude after the three pairing protocols that induced synaptic plasticity. The PPR was transiently decreased after pairing SO 100 ms before SC, which induced synaptic LTP (A). The PPR was transiently increased after pairing SO 10 ms before SC, which induced synaptic STD (B). The PPR was not significantly changed after pairing SC 10 ms before SO, which induced synaptic LTP (C).

Because AChRs in the hippocampus are located both presynaptically and postsynaptically, the contribution of both sites to the various forms of plasticity we have observed was examined by comparing the changes of the paired-pulse ratio (PPR); an increase in the PPR, where the second pulse is increased relative to first pulse, suggests decreased presynaptic release, whereas a decreased ratio suggests increased synaptic release (Dobrunz and Stevens, 1997). For the α7 nAChR-dependent LTP (pairing SO 100 ms before SC), the PPR was decreased initially, and then returned to the baseline (Figure 3A). This suggests that an increased presynaptic release may account for the early potentiation of the EPSCs, but not the late stage. For the α7 nAChR-mediated STD by pairing SO 10 ms before SC, PPR was increased transiently in a time course that fit the time course of the decrease in amplitude of the EPSCs (Figure 3B). This correlation strongly suggests that the STD was mainly mediated through presynaptic inhibition. The PPR was virtually unchanged for the mAChR-mediated LTP (pairing SO 10 ms after SC) (Figure 3C), suggesting that a postsynaptic mechanism is more likely to be mediating this particular form of LTP.

α7 nAChR-Dependent LTP Shares Similar Molecular Mechanisms with NMDA Receptor-Dependent LTP

The molecular mechanisms underlying the α7 nAChR-dependent LTP were further studied. Because the activation of the α7 nAChR is known to mediate calcium influx, we first tested whether intracellular calcium chelation could block this form of LTP. Intracellular dialysis of the CA1 pyramidal neuron with the calcium chelator BAPTA (10 mM) completely blocked this form of LTP (Figure 4A), suggesting a mechanism requiring postsynaptic calcium. Thus, the α7 nAChR activation may act as a source of calcium in inducing this form of LTP. Interestingly, this LTP was also blocked by the NMDAR antagonist AP5 (50 μM) (Figure 4B). Thus, activation of either the α7 nAChR or NMDAR could serve as a source of calcium. Finally, we tested whether this LTP requires the postsynaptic insertion of GluR2-containing AMPARs, which previously have been shown to mediate LTP in hippocampal CA1 spines (Yao et al., 2008). Indeed, dialyzing pyramidal cells with pep2m (100 μM), a peptide containing the NSF (N-ethylmaleimide-sensitive fusion protein)-binding site to GluR2 and, thus, interrupting GluR2-containing AMPAR synaptic insertion, effectively blocked the late stage (about 30 min after the induction of LTP) of the α7 nAChR-dependent LTP (Figure 4C).

To investigate whether the calcium levels in spines might be affected by activation of the α7 nAChR, which in conjunction with the NMDAR induces LTP, we examined the calcium transients in postsynaptic CA1 pyramidal spines using the calcium indicator fluo-4 with two-photon laser-scanning microscopy (Yasuda et al., 2004). SC or SO stimulation alone induced transient calcium increases, which were blocked by the NMDAR antagonist AP5 (Figures 4E and 4F). Neither was blocked by MLA, the α7 nAChR antagonist (Figure 4F), suggesting that α7 nAChR-mediated calcium transients either do not exist or, more likely, were too small to be observed on their own. Interestingly, pairing SO stimulation 100 ms before SC stimulation produced a much longer calcium transient than observed with SC stimulation alone (Figures 4E and 4G). This enhancement was blocked by the α7 nAChR antagonist MLA (Figure 4F). Neither pairing at ±10 ms produced the prolongation of calcium transients. Meanwhile, stimulating the SC twice with an interval of 100 ms also did not produce the prolongation (Figure S2), indicating that it is specifically the pairing of SO 100 ms before the SC that is required. These data show that properly timed α7 nAChR activation prolongs the NMDAR-mediated calcium transients and, thus, induces LTP in an NMDAR-dependent manner, which requires calcium increases in the spines and GluR2-containing AMPAR synaptic insertion.

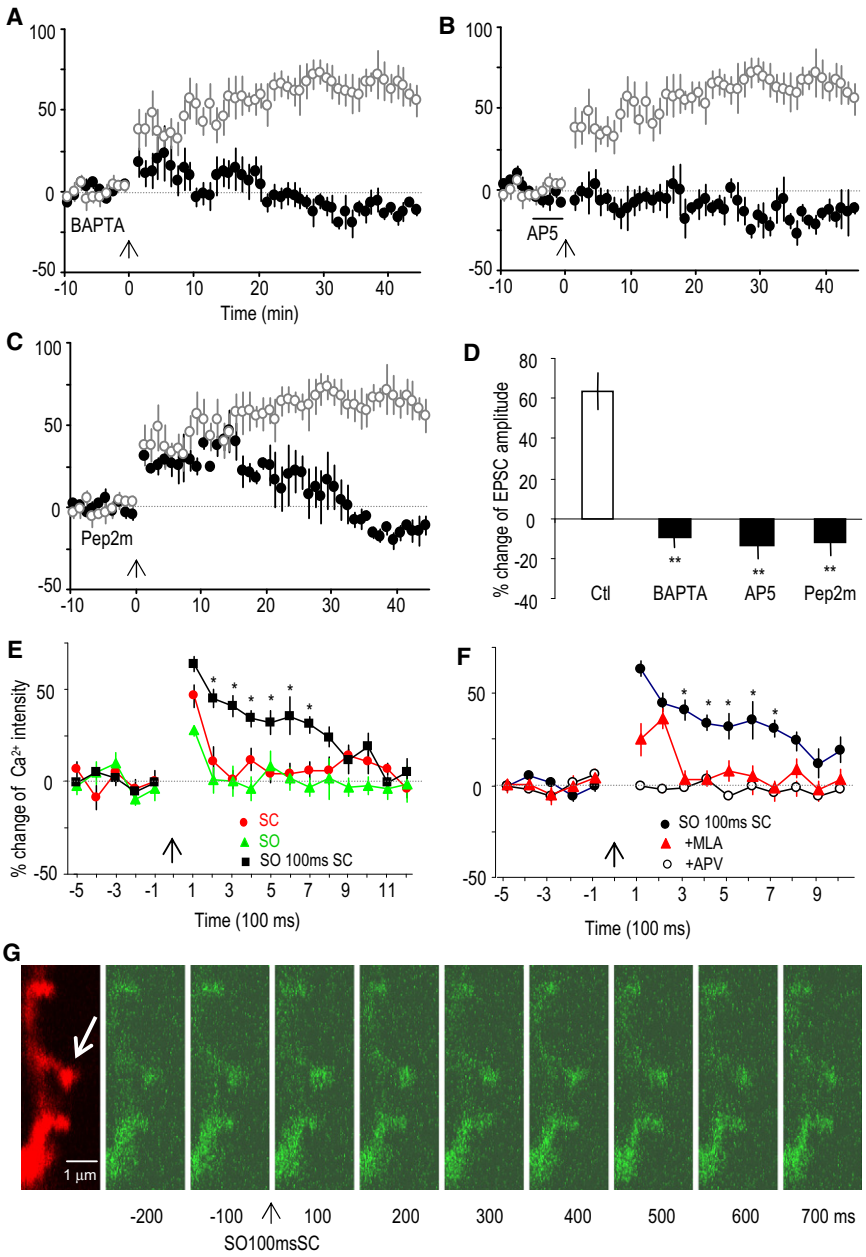

Figure 4. The α7 nAChR-Mediated LTP Involves NMDAR Activation, Intracellular Calcium Increase, and GluR2 AMPAR Synaptic Insertion

(A–C) Percent (%) change of EPSC amplitude showing that the α7 nAChR-mediated LTP (induced by pairing the SO 100 ms before SC) was prevented by (A) including the calcium chelator BAPTA (10 mM) in the recording pipette, (B) the bath application of the NMDA receptor antagonist AP5 (50 μM), and (C) including the peptide pep2m (100 μM) in the recording pipette, which interrupts GluR2 AMPAR synaptic insertion. (D) Bar graph showing the blockage of the LTP by various treatments. **$p < 0.01$, as compared with control (Ctl), Student's t test (n = 5–6). (E) Percent (%) change of calcium intensity showing that stimulating the SC or the SO alone induced only short-term calcium transients, whereas pairing the SO and SC induced prolonged calcium transients. *$p < 0.05$, as compared with SC or SO alone, Student's t test (n = 10–15). Data are shown as mean ± SEM. (F) The enhanced calcium transient induced by pairing SC with SO was blocked by the α7 nAChR antagonist MLA. The calcium transients were completely blocked by NMDAR antagonist AP5. *$p < 0.05$, as compared with MLA or AP5 treatment, Student's t test (n = 10–15). Data are shown as mean ± SEM. (G) Imaging of a segment of dendrite showing the changes in calcium signals in dendritic spines after pairing the SO 100 ms before the SC. The cell was dialyzed with Alexa 594 (red signal) to visualize the spines. The calcium signal was visualized by fluo-4 (green signal). The arrow points to a spine with significant changes in calcium signal after the pairing. See also Figure S2.

Specific Activation of Septal Cholinergic Inputs by an Optogenetic Approach Induces Similar Dynamic Hippocampal Synaptic Plasticity as Induced by Electrical Stimulation

Electrical stimulation of the SO activates not only septal cholinergic inputs but also other local and external inputs, such as glutamatergic inputs in the hippocampus. To address whether septal cholinergic activation alone is sufficient to account for the SO stimulation-induced hippocampal plasticity, an optogenetic approach was used to replace electrical SO stimulation to specifically activate only cholinergic inputs from septal nuclei (Tsai et al., 2009; Witten et al., 2010). To do this, we selectively expressed the light-activated cation channel channelrhodopsin-2 (ChR2) in medial septal cholinergic neurons. Activation of ChR2 with 488 nm light exposure can induce depolarization and action potentials in the neurons expressing this protein. ChR2 is expressed in the soma, dendrites, and axon, and thus, light exposure of the ChR2-expressing axon terminals can induce neurotransmitter release. We injected a Cre-inducible adeno-associated virus (AAV) containing a double-floxed inverted ChR2 (Tsai et al., 2009; Witten et al., 2010) into the medial septal nuclei of choline acetyltransferase (ChAT)-Cre transgenic mice. This Cre-inducible AAV is only expressed in Cre-expressing cells (in this case the cholinergic neurons; i.e., the ChAT-positive cells) because the Cre expression is driven by the ChAT promoter. Selective expression of ChR2 (fused with mCherry) in septal cholinergic (ChAT-positive) neurons was verified by immunohistochemistry (Figures 5A–5C). Functional expression of ChR2 was verified by inducing action potentials with 488 nm laser light exposure of cell bodies or nearby dendrites (Figures S3A and S3B). Septal cholinergic projections in the hippocampus visualized by mCherry showed axons coming from the fimbria/fornix branch in the SO (Figures 5D–5H). Many of these

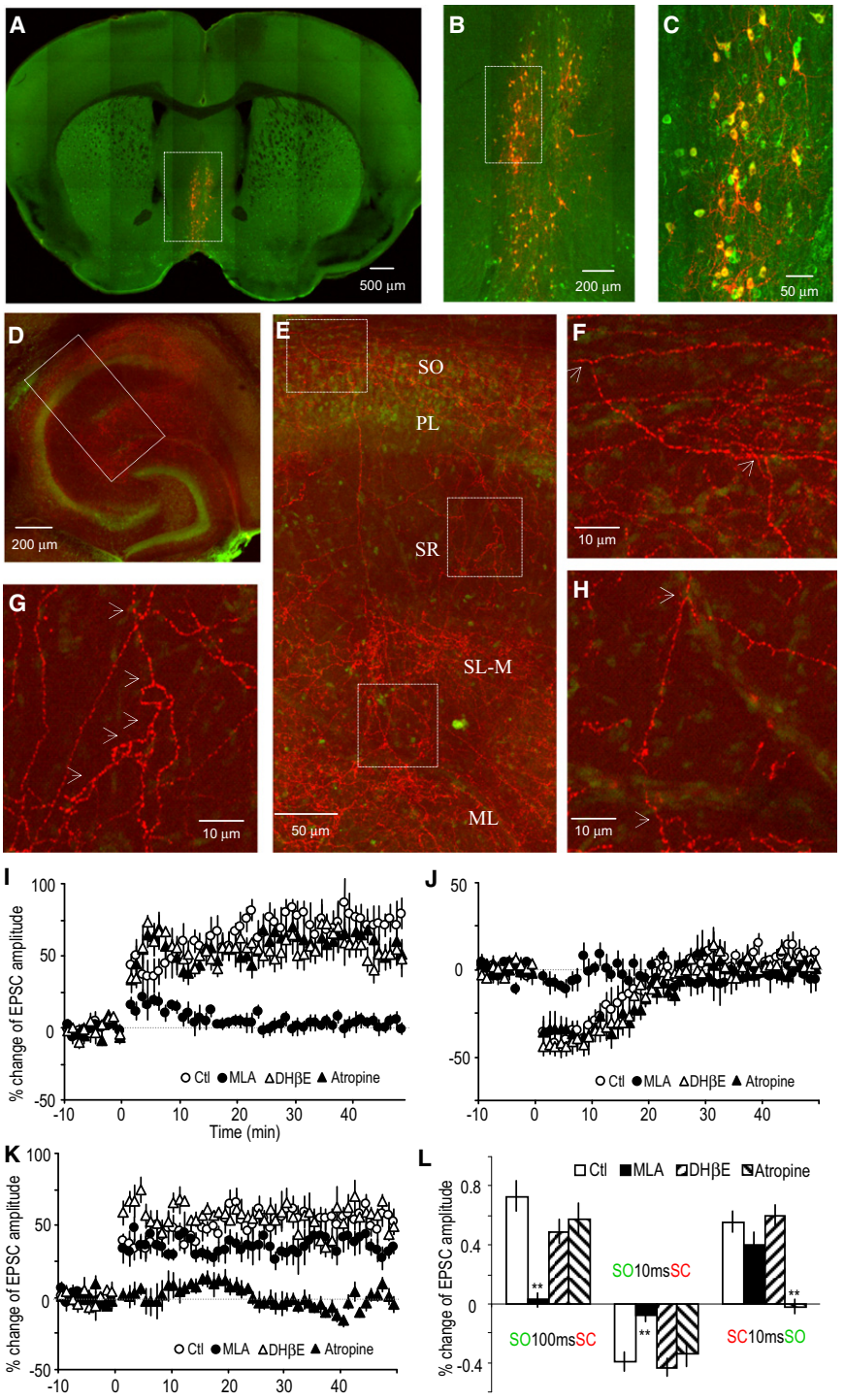

Figure 5. Optogenetically Activated Cholinergic Inputs Induce Dynamic Synaptic Plasticity of SC-CA1 Synapses

(A–C) Immunostaining of ChAT (green) in a coronal section of medial septum showing that ChR2 (fused with mCherry, shown in red) was expressed exclusively in medial septal ChAT-positive neurons. Squares in (A) and (B) define the regions shown in (B) and (C), respectively. (D) Horizontal hippocampal slice showing the abundant presence of ChR2-expressing cholinergic terminals (mCherry, red) in hippocampus. The pyramidal layer is visualized with NeuroTrace fluorescent Nissl stain (green). Square defines the region shown in (E). (E) Inset from (D) showing the distribution of cholinergic terminals in different cell layers in (and near) the CA1 region. Squares define the regions shown in (F)–(H), respectively, from up to down. (F–H) Insets from (E) showing the bifurcation (indicated by arrowheads) of the cholinergic terminals, suggesting that the primary branches originated in the SO layer. The axon shown in (H) is extended from that in (F). PL, pyramidal cell layer; SL-M, stratum lacunosum-moleculare; ML, molecular layer of dentate gyrus. (I) LTP was induced by optically activating the cholinergic input 100 ms before stimulating the SC, which was prevented by the α7 nAChR antagonist MLA, but not by the non-α7 nAChR antagonist DHβE or the mAChR antagonist atropine. (J) STD was induced by activating the cholinergic input 10 ms before the SC, which was also prevented by MLA, but not by DHβE or atropine. (K) LTP was induced by pairing the SC 10 ms before optically activating the cholinergic input, which was prevented by atropine, but not by MLA or DHβE. (L) Bar graph showing the three types of synaptic plasticity and the effects of the three AChR antagonists on the plasticity, respectively. **$p < 0.01$, as compared with control, Student's t test ($n = 5–6$ in each group). Data are shown as mean ± SEM. See also Figure S3.

axon projections send branches to deeper layers of the stratum radiatum, stratum lacunosum-moleculare, and the molecular layer of the dentate gyrus. This pattern confirms our presumption that the upstream primary cholinergic branches innervating the CA1 are located in the SO and supports our use of SO stimulation to activate cholinergic inputs, either electrically or optically, to the CA1.

To activate the cholinergic inputs to the CA1, cholinergic terminals in a small region of the SO were exposed to 488 nm light for 20 ms. Activation of the terminals sometimes induced visible nAChR-mediated currents in about 20% of the pyramidal neurons (Figure S3E), usually with a 20 ms delay between the time of light exposure and the cholinergic response. Three time intervals pairing light exposure with SC stimulation were selected to mimic the corresponding pairings of SO and SC electrical stimulation that produced the observed three types of synaptic plasticity described above. Consistent with the results from electrical SO stimulation, when cholinergic input was activated 100 ms (i.e., light exposure 120 ms to take into account the 20 ms delay) before SC stimulation, LTP was induced, which was blocked by the α7 nAChR antagonist MLA, but not by DHβE or atropine (Figures 5I and

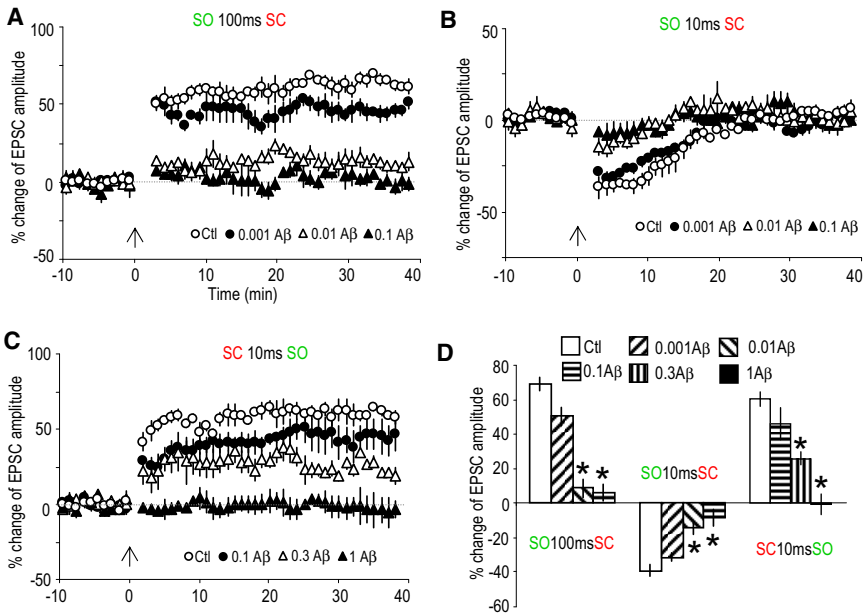

Figure 6. Aβ Differentially Impaired α7 nAChR- and mAChR-Mediated Synaptic Plasticity

(A–C) Percent (%) change of EPSC amplitude showing the effects of 2 hr pre-exposure to various doses of Aβ on the three types of plasticity. Both of the α7 nAChR-mediated LTP (A) and STD (B) were largely blocked by Aβ at a concentration as low as 0.01 μM. The mAChR-mediated LTP (C) was partially blocked by 0.3 μM Aβ and completely blocked by 1 μM Aβ. (D) Bar graph showing the effects of Aβ at various concentrations on the three types of synaptic plasticity. *p < 0.001, as compared with no Aβ treatment, Student's t test (n = 5–7). Data are shown as mean ± SEM.

5H). When cholinergic input was activated 10 ms before SC stimulation, STD was induced, which was also sensitive to MLA, but not to DHβE or atropine (Figures 5J and 5H). When cholinergic input was activated 10 ms after SC stimulation, LTP was induced, which was blocked by atropine, but not by MLA or DHβE (Figures 5K and 5L). These results demonstrate that cholinergic input alone, activated by either SO stimulation or by light in cholinergic neurons expressing ChR2, is sufficient to induce the various forms of timing-dependent synaptic plasticity.

α7 nAChR-Dependent Synaptic Plasticity Is More Vulnerable to Aβ Exposure than mAChR-Dependent Synaptic Plasticity

We then investigated the potential implication of this synaptic plasticity in higher cognitive functions. Cholinergic dysfunction has long been hypothesized to be a major cause for the cognitive deficit in AD (Bartus et al., 1982; Terry and Buccafusco, 2003). Recent studies strongly suggest that the soluble oligomeric rather than the fibrillar form of β-amyloid (Aβ) causes synaptic and cognitive dysfunction in AD, and the underlying mechanisms have, therefore, been the focus of current studies (Lue et al., 1999; McLean et al., 1999; Selkoe, 2002; Hsieh et al., 2006; Haass and Selkoe, 2007). Here, we show that the α7 nAChR-dependent LTP and STD were largely blocked in slices pre-exposed to 10 nM Aβ for 2 hr (Figures 6A, 6B, and 6D); our Aβ preparation contains oligomeric, as well as monomeric, Aβ (Lambert et al., 1998). The mAChR-mediated LTP is relatively resistant to 0.1 μM Aβ but was blocked by higher concentrations of Aβ pre-exposure (partial blockade by 0.3 and complete blockade by 1 μM) (Figures 6C and 6D).

Thus, these results provide a mechanism for Aβ to impair cholinergic-related synaptic plasticity and cognitive functions. On the other hand, we have recently shown that a dual allosteric modulator, which can simultaneously enhance α7 nAChRs and inhibit α5 subunit-containing γ-aminobutyric acid (GABAergic) receptors, not only induces LTP in hippocampal slices but also enhances performance in the radial arm maze and facilitates attentional states in the five-choice serial reaction time trial in animals (Johnstone et al., 2011); presumably, this is achieved by increasing the possibility of properly timed spontaneous cholinergic and glutamatergic synaptic transmission in the hippocampus. These results strongly suggest that the cholinergic-mediated synaptic plasticity is closely related to cognitive performance, and provides a relevant platform for further testing therapeutic compounds for hippocampus-based cognitive impairment including AD.

DISCUSSION

Multiple forms of synaptic plasticity have previously been shown to be regulated by both nAChR and mAChR activation. For the nAChRs (and in particular the α7 subtype), the activation of receptors with exogenous ligands in the CA1 and dentate regions enhanced synaptic plasticity (Fujii et al., 1999; Mann and Greenfield, 2003; Welsby et al., 2006; Welsby et al., 2007). Furthermore, the effect that the activation of these receptors has on synaptic plasticity can depend on the location of the receptors as well as timing; for example the activation of α7 nAChRs on hippocampal interneurons can block concurrent STP and LTP in pyramidal cells, whereas presynaptic nAChRs can enhance the release of glutamate and, thus, increase the probability of inducing LTP (Ji et al., 2001). In addition exogenous ACh may convert HFS-induced STP to LTP or LTD, depending on the timing relative to the SC stimulation (Ge and Dani, 2005). Our current study is in large part consistent with these conclusions, stressing the importance of proper timing of cholinergic activation in shaping hippocampal synaptic plasticity. We have also recently shown that nicotine, acting through the non-α7 nAChRs, was able to enhance synaptic plasticity in deep layers of the entorhinal cortex (Tu et al., 2009). This is consistent with a recent report that α4-containing nAChRs contribute to LTP facilitation in the perforant path (Nashmi et al., 2007). Multiple forms of synaptic plasticity can also be regulated by mAChRs (Maylie and Adelman, 2010). For example, the activation of

presynaptic or postsynaptic mAChRs has previously been shown to either enhance or reduce LTP in the hippocampus (Leung et al., 2003; Ovsepian et al., 2004; Seeger et al., 2004; Cobb and Davies, 2005). Recently, it was shown that endogenous ACh, acting through the M1 mAChR subtype, facilitates LTP in the hippocampus via inhibition of SK channels (Buchanan et al., 2010).

Here, we show that the septal cholinergic input can directly induce hippocampal synaptic plasticity in a timing-dependent manner. When the cholinergic input to the CA1 was activated 100 or 10 ms prior to the SC stimulation, it resulted in α7 nAChR-dependent LTP or STD, respectively. This α7 nAChR-dependent LTP was likely due to a postsynaptic effect that required the activation of the NMDAR and prolongation of the NMDAR-mediated calcium transients in the spines, and GluR2-containing AMPAR synaptic insertion. The α7 nAChR-dependent STD appears to be mediated primarily through the presynaptic inhibition of glutamate release (Figure 3). The third and last form of plasticity that we observed was when the cholinergic stimulation was given 10 ms *after* the SC stimulation; this induced LTP that was dependent on the activation of the mAChR. The underlying mechanism is not clear at this time. PPR study suggests a postsynaptic mechanism (Figure 3), but we have not been able to block this LTP with a calcium chelator dialyzed into the cells under recording (data not shown).

The majority of modulatory transmitter receptors are G protein-coupled receptors that exert functions through intracellular signaling pathways and are, thus, considered slow synaptic transmission mediators, as opposed to those receptors that are ligand-gated ion channels (Greengard, 2001). Previous studies have focused on the modulatory effects on existing HFS-induced hippocampal synaptic plasticity by either nAChR or mAChR activation. Our study here clearly shows that cholinergic input, through either its ion channel receptor (α7 nAChR) or the G protein-coupled receptor (mAChR), can directly induce hippocampal synaptic plasticity in a timing- and context-dependent manner. With timing shifts in the millisecond range, different types of synaptic plasticity are induced through different AChR subtypes with different mechanisms (presynaptic or postsynaptic). Thus, these results have revealed the striking temporal accuracy of modulatory transmitter systems and the subsequent complex functions achieved based on this capability.

This study also reveals novel physiologically reasonable neural activity patterns that induce synaptic plasticity, a very important question in learning and memory studies (Kandel, 2009). The HFS-induced synaptic plasticity has provided valuable information in underlying molecular mechanisms but has been questioned as a physiological firing pattern. For this reason, spike timing-dependent plasticity is considered physiologically more reasonable (Markram et al., 1997; Kandel, 2009). Even so, both models focus on manipulating the firing patterns of the same glutamatergic pathway where synaptic plasticity will form. In the present study synaptic plasticity is induced by an extrinsic input and, thus, provides a mechanism to integrate information from extrinsic pathways and store it in local synapses. Thus, it is more relevant to understanding learning and memory, which always involve the precise coordination among multiple brain regions.

Cognitive deficits in AD have long been thought to be caused in part by cholinergic dysfunction (Bartus et al., 1982; Terry and Buccafusco, 2003). Here, we have shown that concentrations of oligomeric Aβ as low as 10 nM largely blocks both forms of α7 nAChR-dependent plasticity. For the mAChR-mediated LTP, a concentration of Aβ of nearly 1 μM is required to block this form of plasticity; this concentration is comparable to those who previously have studied Aβ inhibition of hippocampal synaptic plasticity (Lambert et al., 1998; Vitolo et al., 2002; Wang et al., 2004). The synthetic Aβ is much less efficient than naturally secreted Aβ (about 0.5%) in inhibiting hippocampal LTP (Wang et al., 2004). The fact that the α7 nAChR-dependent plasticity is more sensitive to Aβ may be due to the previously reported ability of Aβ to bind to the α7 nAChR with high affinity. However, the sensitivity of α7 nAChRs to Aβ may vary due to its coassembly with other subunits and/or among different neuronal populations (Liu et al., 2001, 2009; Pettit et al., 2001), and Aβ may be exerting its effect on plasticity through other mechanisms (Nimmrich et al., 2008). Thus, nevertheless, these results provide a mechanism for Aβ to impair cholinergic-related synaptic plasticity and cognitive functions, and provide a relevant platform for further testing therapeutic compounds for cholinergic-dependent cognitive impairment including AD.

EXPERIMENTAL PROCEDURES

Animals and Chemicals

Rats were obtained from Charles River Laboratories. α7 nAChR KO mice and ChAT-Cre transgenic mice were obtained from Jackson Laboratory. Mice were ear-punched and genotyped at day 19 and used for experiments from day 21. All procedures were approved and performed in compliance with NIEHS/NIH Humane Care and Use of Animals in Research protocols. Unless otherwise indicated, general chemicals or drugs were obtained from Sigma, and fluorescent materials were from Invitrogen. pep2m was from Tocris.

Slice Preparation and Whole-Cell Patch-Clamp Recordings

Animals (2- to 3-week-old Wistar rats, 3- to 4-week-old α7 nAChR KO mice, and 5- to 6-week-old ChAT-Cre transgenic mice) were anesthetized with isoflurane and decapitated. Brains were quickly dissected and placed into carboxygenated (95%O_2/5%CO_2) ice-cold artificial cerebral spinal fluid (ACSF) containing 122 mM NaCl, 2.5 mM KCl, 1.3 mM $MgCl_2$, 2 mM $CaCl_2$, 1.2 mM NaH_2PO_4, 25 mM $NaHCO_3$, and 25 mM glucose. Horizontal brain slices (300 μm) corresponding to plate 190–200 of the Paxinos rat brain atlas (Paxinos and Watson, 2007) were cut with a vibratome (Leica; VT1000S). Slices were then stored in ACSF continuously bubbled with carboxygen at room temperature (RT) for more than 1 hr before use.

Slices used for whole-cell patch-clamp studies were continuously perfused with ACSF in a submerged chamber at a rate of 2 ml/min. Whole-cell patch clamp was performed under guidance of IR-DIC optics using an Axopatch 200B patch amplifier (Axon Instruments) with a glass pipette filled with an internal solution containing 120 mM potassium gluconate (KGluc), 2 mM NaCl, 5 mM MgATP, 0.3 mM Na_2GTP, 20 mM KCl, 10 mM HEPES, 1 mM EGTA, and 11.3 mM D-glucose, with pH ~7.2–7.3 and osmolarity of ~270–280 mOsm. Series resistances ranging from 7 to 40 MΩ were not compensated for during recordings but were monitored throughout the experiments. Recordings were discarded when a significant (>20%) change of series resistance was detected. Data were digitized with Digidata 1322A, collected with CLAMPEX, and analyzed with Clampfit. EPSCs were recorded under voltage clamp at −60 mV.

Pairing Two Input Pathways by Electrical Stimulation

Evoked EPSCs were recorded from hippocampal CA1 pyramidal neurons by electrically stimulating the SC pathway. Cholinergic terminals were activated

by electrically stimulating the SO. The stimulation intensity was adjusted to evoke a postsynaptic current of about 50–100 pA in amplitude, and the intensity was usually around 20–100 μA for 0.1 ms for SC and 50–200 μA for SO pathway. For LTP the amplitude of EPSCs at the 40 min time point after the pairing protocol was compared with that before the pairing protocol. For STD the amplitude at the 5 min time point after pairing was compared with before. Bath-applied cholinergic receptor antagonists or other chemicals were applied 5 min before and during the pairing protocol, and were washed away immediately after the pairing procedure.

Calcium Imaging in Dendritic Spines

Calcium imaging was done with the calcium indicator fluo-4 (200 μM included in recording pipette). Alexa 594 (100 μM) was also included in the recording pipette to visualize the dendrites of neurons under recording. Images were acquired with a Zeiss LSM 510 NLO META system coupled to an Axioskop 2FS microscope (Carl Zeiss, Inc., Thornwood, NY, USA) using a Ti:sapphire Chameleon two-photon laser system (Coherent, Inc., Auburn, CA, USA). A wavelength of 810 nm was used to excite both fluo-4 and Alexa 594. An IR Achroplan 63× objective lens (N.A. 1.1) was used. Emissions were collected using band-pass filters BP 500–550 IR and BP 640–720 IR, respectively (Chroma Technology Corp., Rockingham, VT, USA). Image acquisition and online analysis were performed using Zeiss LSM 510 software.

Stereotaxic Injection of Viruses into Medial Septum in Mice

ChR2 was expressed in the medial septum in ChAT-Cre mice (expressing Cre under ChAT promoter). AAV-FLEX-rev-ChR2(H134R)-mCherry carrying double-floxed ChR2 with reversed sequence (Addgene plasmid 20297 from Karl Deisseroth) was packaged with AAV serotype 9 by the virus core facility at NIEHS. Virus (0.5 μl) was injected into 21-day-old mice (anesthetized with 75 mg/kg ketamine and 7.5 mg/kg xylazine) with the following coordinates: bregma, 0.5 mm; lateral, 0.3 mm tilted at 8° toward the midline; and dorsal-ventral, 4.0 mm. Animals were allowed to recover for at least 12 days, and then hippocampal slices for recordings were prepared as described above.

Activating ChR2-Expressing Cholinergic Neurons by Light Exposure

The Zeiss LSM 510 NLO META system was also used to generate the light to activate ChR2-expressing cholinergic terminals in the hippocampal SO region, which was coexpressed with mCherry and visualized with 543 nm light that does not activate ChR2. ChR2 was activated with 488 nm laser. The exposure time, intensity, and area were controlled by the LSM 510 system. The intensity of the light used to activate ChR2 in processes was usually 7.5 mW for 20 ms. The cholinergic response (nAChR-mediated currents in CA1 neurons) was usually induced at around 20 ms after initiating the light exposure. To achieve a 100 ms interval for cholinergic inputs before SC inputs, the light exposure was set at 120 ms before SC input.

Immunohistochemistry

Coronal slices (100 μm) of medial septum or horizontal slices of hippocampus were cut from 4% paraformaldehyde-fixed brains. After blocking with 5% bovine serum albumin for 1 hr at RT, medial septal slices were incubated with goat anti-ChAT antibody (Chemicon; 1:200) at 4°C for 48 hr, and then incubated with secondary Alexa 488-conjugated donkey anti-goat antibody (1:200) for 4 hr at RT. The hippocampal slices were incubated with NeuroTrace fluorescent Nissl stain (1:300) for 2 hr at RT to locate the pyramidal layer. Images were then taken with Zeiss LSM 710 Zen system.

Aβ Treatment

Human Aβ (1-42) peptide was purchased from AnaSpec. It was dissolved in 1% NH_4OH at 3 mM. Aliquots were stored at −20°C. Oligomeric Aβ was produced by diluting the stock solution with PBS to 0.1 mM and incubated at 4°C for 48 hr (Lambert et al., 1998). This preparation also contains monomeric Aβ. After brief centrifugation, the supernatant was used to treat hippocampal slices for 2–4 hr before the recording experiments.

Statistics

For whole-cell recordings the amplitude of SC-EPSC was analyzed with Clampfit. The percent (%) changes were calculated by comparing with the average of 10 min baseline recording. For calcium imaging the averages of 500 ms baseline (five time points) were used to calculate the percent (%) changes. Values were always presented as mean ± SEM. Two-tailed Student's t tests were performed to compare changes with the baselines or controls.

SUPPLEMENTAL INFORMATION

Supplemental Information includes Supplemental Experimental Procedures and three figures and can be found online at doi:10.1016/j.neuron.2011.04.026.

ACKNOWLEDGMENTS

We thank Patricia Lamb for animal genotyping and plasmid preparation, Drs. Negin Martin and Charles Romeo for virus packaging, Dr. James M. Wilson at University of Pennsylvania for providing the AAV serotype 9 helper plasmid, and Charles J. Tucker and Agnus Janoshazi for assistance with fluorescent microscopy. We also thank Drs. Serena Dudek, David Armstrong, Patricia Jensen, and Lutz Birnbaumer for discussions and critical reading of the manuscript. This research was supported by the Intramural Research Program of the NIH, National Institute of Environmental Health Sciences.

Accepted: April 13, 2011
Published: July 13, 2011

REFERENCES

Bartus, R.T., Dean, R.L., 3rd, Beer, B., and Lippa, A.S. (1982). The cholinergic hypothesis of geriatric memory dysfunction. Science *217*, 408–414.

Bliss, T.V., and Collingridge, G.L. (1993). A synaptic model of memory: long-term potentiation in the hippocampus. Nature *361*, 31–39.

Buchanan, K.A., Petrovic, M.M., Chamberlain, S.E., Marrion, N.V., and Mellor, J.R. (2010). Facilitation of long-term potentiation by muscarinic M(1) receptors is mediated by inhibition of SK channels. Neuron *68*, 948–963.

Cobb, S.R., and Davies, C.H. (2005). Cholinergic modulation of hippocampal cells and circuits. J. Physiol. *562*, 81–88.

Cole, A.E., and Nicoll, R.A. (1983). Acetylcholine mediates a slow synaptic potential in hippocampal pyramidal cells. Science *221*, 1299–1301.

Cole, A.E., and Nicoll, R.A. (1984). Characterization of a slow cholinergic post-synaptic potential recorded in vitro from rat hippocampal pyramidal cells. J. Physiol. *352*, 173–188.

Dan, Y., and Poo, M.M. (2004). Spike timing-dependent plasticity of neural circuits. Neuron *44*, 23–30.

Dani, J.A., and Bertrand, D. (2007). Nicotinic acetylcholine receptors and nicotinic cholinergic mechanisms of the central nervous system. Annu. Rev. Pharmacol. Toxicol. *47*, 699–729.

Dobrunz, L.E., and Stevens, C.F. (1997). Heterogeneity of release probability, facilitation, and depletion at central synapses. Neuron *18*, 995–1008.

Dutar, P., Bassant, M.H., Senut, M.C., and Lamour, Y. (1995). The septohippocampal pathway: structure and function of a central cholinergic system. Physiol. Rev. *75*, 393–427.

Fujii, S., Ji, Z., Morita, N., and Sumikawa, K. (1999). Acute and chronic nicotine exposure differentially facilitate the induction of LTP. Brain Res. *846*, 137–143.

Ge, S., and Dani, J.A. (2005). Nicotinic acetylcholine receptors at glutamate synapses facilitate long-term depression or potentiation. J. Neurosci. *25*, 6084–6091.

Gradinaru, V., Zhang, F., Ramakrishnan, C., Mattis, J., Prakash, R., Diester, I., Goshen, I., Thompson, K.R., and Deisseroth, K. (2010). Molecular and cellular approaches for diversifying and extending optogenetics. Cell *141*, 154–165.

Greengard, P. (2001). The neurobiology of slow synaptic transmission. Science *294*, 1024–1030.

Haass, C., and Selkoe, D.J. (2007). Soluble protein oligomers in neurodegeneration: lessons from the Alzheimer's amyloid beta-peptide. Nat. Rev. Mol. Cell Biol. *8*, 101–112.

Hsieh, H., Boehm, J., Sato, C., Iwatsubo, T., Tomita, T., Sisodia, S., and Malinow, R. (2006). AMPAR removal underlies Abeta-induced synaptic depression and dendritic spine loss. Neuron *52*, 831–843.

Jerusalinsky, D., Kornisiuk, E., and Izquierdo, I. (1997). Cholinergic neurotransmission and synaptic plasticity concerning memory processing. Neurochem. Res. *22*, 507–515.

Ji, D., Lape, R., and Dani, J.A. (2001). Timing and location of nicotinic activity enhances or depresses hippocampal synaptic plasticity. Neuron *31*, 131–141.

Johnstone, T.B., Gu, Z., Yoshimura, R.F., Villegier, A.S., Hogenkamp, D.J., Whittemore, E.R., Huang, J.C., Tran, M.B., Belluzzi, J.D., Yakel, J.L., and Gee, K.W. (2011). Allosteric modulation of related ligand-gated ion channels synergistically induces long-term potentiation in the hippocampus and enhances cognition. J. Pharmacol. Exp. Ther. *336*, 908–915.

Kandel, E.R. (2009). The biology of memory: a forty-year perspective. J. Neurosci. *29*, 12748–12756.

Kenney, J.W., and Gould, T.J. (2008). Modulation of hippocampus-dependent learning and synaptic plasticity by nicotine. Mol. Neurobiol. *38*, 101–121.

Lambert, M.P., Barlow, A.K., Chromy, B.A., Edwards, C., Freed, R., Liosatos, M., Morgan, T.E., Rozovsky, I., Trommer, B., Viola, K.L., et al. (1998). Diffusible, nonfibrillar ligands derived from Abeta1-42 are potent central nervous system neurotoxins. Proc. Natl. Acad. Sci. USA *95*, 6448–6453.

Leung, L.S., Shen, B., Rajakumar, N., and Ma, J. (2003). Cholinergic activity enhances hippocampal long-term potentiation in CA1 during walking in rats. J. Neurosci. *23*, 9297–9304.

Liu, Q., Kawai, H., and Berg, D.K. (2001). beta -Amyloid peptide blocks the response of alpha 7-containing nicotinic receptors on hippocampal neurons. Proc. Natl. Acad. Sci. USA *98*, 4734–4739.

Liu, Q., Huang, Y., Xue, F., Simard, A., DeChon, J., Li, G., Zhang, J., Lucero, L., Wang, M., Sierks, M., et al. (2009). A novel nicotinic acetylcholine receptor subtype in basal forebrain cholinergic neurons with high sensitivity to amyloid peptides. J. Neurosci. *29*, 918–929.

Lue, L.F., Kuo, Y.M., Roher, A.E., Brachova, L., Shen, Y., Sue, L., Beach, T., Kurth, J.H., Rydel, R.E., and Rogers, J. (1999). Soluble amyloid beta peptide concentration as a predictor of synaptic change in Alzheimer's disease. Am. J. Pathol. *155*, 853–862.

Malenka, R.C. (2003). Synaptic plasticity and AMPA receptor trafficking. Ann. N Y Acad. Sci. *1003*, 1–11.

Mann, E.O., and Greenfield, S.A. (2003). Novel modulatory mechanisms revealed by the sustained application of nicotine in the guinea-pig hippocampus in vitro. J. Physiol. *551*, 539–550.

Markram, H., Lübke, J., Frotscher, M., and Sakmann, B. (1997). Regulation of synaptic efficacy by coincidence of postsynaptic APs and EPSPs. Science *275*, 213–215.

Maylie, J., and Adelman, J.P. (2010). Cholinergic signaling through synaptic SK channels: it's a protein kinase but which one? Neuron *68*, 809–811.

McLean, C.A., Cherny, R.A., Fraser, F.W., Fuller, S.J., Smith, M.J., Beyreuther, K., Bush, A.I., and Masters, C.L. (1999). Soluble pool of Abeta amyloid as a determinant of severity of neurodegeneration in Alzheimer's disease. Ann. Neurol. *46*, 860–866.

Nashmi, R., Xiao, C., Deshpande, P., McKinney, S., Grady, S.R., Whiteaker, P., Huang, Q., McClure-Begley, T., Lindstrom, J.M., Labarca, C., et al. (2007). Chronic nicotine cell specifically upregulates functional alpha 4* nicotinic receptors: basis for both tolerance in midbrain and enhanced long-term potentiation in perforant path. J. Neurosci. *27*, 8202–8218.

Nimmrich, V., Grimm, C., Draguhn, A., Barghorn, S., Lehmann, A., Schoemaker, H., Hillen, H., Gross, G., Ebert, U., and Bruehl, C. (2008). Amyloid beta oligomers (A beta(1-42) globulomer) suppress spontaneous synaptic activity by inhibition of P/Q-type calcium currents. J. Neurosci. *28*, 788–797.

Ovsepian, S.V., Anwyl, R., and Rowan, M.J. (2004). Endogenous acetylcholine lowers the threshold for long-term potentiation induction in the CA1 area through muscarinic receptor activation: in vivo study. Eur. J. Neurosci. *20*, 1267–1275.

Paxinos, G., and Watson, C. (2007). The Rat Brain in Stereotaxic Coordinates, Sixth Edition (San Diego, CA: Academic Press).

Pettit, D.L., Shao, Z., and Yakel, J.L. (2001). beta-Amyloid(1-42) peptide directly modulates nicotinic receptors in the rat hippocampal slice. J. Neurosci. *21*, RC120.

Power, A.E., Vazdarjanova, A., and McGaugh, J.L. (2003). Muscarinic cholinergic influences in memory consolidation. Neurobiol. Learn. Mem. *80*, 178–193.

Reis, H.J., Guatimosim, C., Paquet, M., Santos, M., Ribeiro, F.M., Kummer, A., Schenatto, G., Salgado, J.V., Vieira, L.B., Teixeira, A.L., and Palotás, A. (2009). Neuro-transmitters in the central nervous system & their implication in learning and memory processes. Curr. Med. Chem. *16*, 796–840.

Seeger, T., Fedorova, I., Zheng, F., Miyakawa, T., Koustova, E., Gomeza, J., Basile, A.S., Alzheimer, C., and Wess, J. (2004). M2 muscarinic acetylcholine receptor knock-out mice show deficits in behavioral flexibility, working memory, and hippocampal plasticity. J. Neurosci. *24*, 10117–10127.

Selkoe, D.J. (2002). Alzheimer's disease is a synaptic failure. Science *298*, 789–791.

Silberberg, G., Wu, C., and Markram, H. (2004). Synaptic dynamics control the timing of neuronal excitation in the activated neocortical microcircuit. J. Physiol. *556*, 19–27.

Terry, A.V., Jr., and Buccafusco, J.J. (2003). The cholinergic hypothesis of age and Alzheimer's disease-related cognitive deficits: recent challenges and their implications for novel drug development. J. Pharmacol. Exp. Ther. *306*, 821–827.

Tsai, H.C., Zhang, F., Adamantidis, A., Stuber, G.D., Bonci, A., de Lecea, L., and Deisseroth, K. (2009). Phasic firing in dopaminergic neurons is sufficient for behavioral conditioning. Science *324*, 1080–1084.

Tu, B., Gu, Z., Shen, J.X., Lamb, P.W., and Yakel, J.L. (2009). Characterization of a nicotine-sensitive neuronal population in rat entorhinal cortex. J. Neurosci. *29*, 10436–10448.

Vitolo, O.V., Sant'Angelo, A., Costanzo, V., Battaglia, F., Arancio, O., and Shelanski, M. (2002). Amyloid beta -peptide inhibition of the PKA/CREB pathway and long-term potentiation: reversibility by drugs that enhance cAMP signaling. Proc. Natl. Acad. Sci. USA *99*, 13217–13221.

Wanaverbecq, N., Semyanov, A., Pavlov, I., Walker, M.C., and Kullmann, D.M. (2007). Cholinergic axons modulate GABAergic signaling among hippocampal interneurons via postsynaptic α 7 nicotinic receptors. J. Neurosci. *27*, 5683–5693.

Wang, Q., Rowan, M.J., and Anwyl, R. (2004). Beta-amyloid-mediated inhibition of NMDA receptor-dependent long-term potentiation induction involves activation of microglia and stimulation of inducible nitric oxide synthase and superoxide. J. Neurosci. *24*, 6049–6056.

Welsby, P., Rowan, M., and Anwyl, R. (2006). Nicotinic receptor-mediated enhancement of long-term potentiation involves activation of metabotropic glutamate receptors and ryanodine-sensitive calcium stores in the dentate gyrus. Eur. J. Neurosci. *24*, 3109–3118.

Welsby, P.J., Rowan, M.J., and Anwyl, R. (2007). Beta-amyloid blocks high frequency stimulation induced LTP but not nicotine enhanced LTP. Neuropharmacology *53*, 188–195.

Widmer, H., Ferrigan, L., Davies, C.H., and Cobb, S.R. (2006). Evoked slow muscarinic acetylcholinergic synaptic potentials in rat hippocampal interneurons. Hippocampus *16*, 617–628.

Witten, I.B., Lin, S.C., Brodsky, M., Prakash, R., Diester, I., Anikeeva, P., Gradinaru, V., Ramakrishnan, C., and Deisseroth, K. (2010). Cholinergic interneurons control local circuit activity and cocaine conditioning. Science *330*, 1677–1681.

Yao, Y., Kelly, M.T., Sajikumar, S., Serrano, P., Tian, D., Bergold, P.J., Frey, J.U., and Sacktor, T.C. (2008). PKM ζ maintains late long-term potentiation by N-ethylmaleimide-sensitive factor/GluR2-dependent trafficking of postsynaptic AMPA receptors. J. Neurosci. *28*, 7820–7827.

Yasuda, R., Nimchinsky, E.A., Scheuss, V., Pologruto, T.A., Oertner, T.G., Sabatini, B.L., and Svoboda, K. (2004). Imaging calcium concentration dynamics in small neuronal compartments. Sci. STKE *2004*, pl5.

Zhang, J., and Berg, D.K. (2007). Reversible inhibition of GABAA receptors by α7-containing nicotinic receptors on the vertebrate postsynaptic neurons. J. Physiol. *579*, 753–763.

Zhang, L.I., Tao, H.W., Holt, C.E., Harris, W.A., and Poo, M. (1998). A critical window for cooperation and competition among developing retinotectal synapses. Nature *395*, 37–44.